



ELSEVIER

Available online at www.sciencedirect.com

ScienceDirect

journal homepage: www.elsevier.com/locate/he

Vapor pressure measurements of $\text{Mg}(\text{BH}_4)_2$ using Knudsen torsion effusion thermo graphic method

L.-N.N. Nforbi^a, A. Talekar^a, K.H. Lau^c, R. Chellapa^b, W.-M. Chien^a,
D. Chandra^{a,*}, H. Hagemann^d, Y. Filinchuk^g, J.-C. Zhao^e,
Andre Levchenko^f

^a Metallurgy and Materials Sciences, MS 388, University of Nevada, Reno, NV 89557, USA

^b Shock & Detonation Physics (WX-9), MS H805, Los Alamos National Laboratory, Los Alamos, NM 87545, USA

^c SRI International, 333 Ravenswood Avenue, Menlo Park, CA 94025, USA

^d University of Geneva, Chemistry Dept., Quai Ernest-Ansermet 24, CH-1211 Genève 4, Switzerland

^e Ohio State University, 477 Watts Hall, 2041 College Rd., Columbus, OH 43210, USA

^f Setaram Inc., 8430 Central Ave., Suite C, Newark, CA 94560, USA

^g Université Catholique de Louvain (UCL), Place Louis Pasteur 1, 1348 Louvain-la-Neuve, Belgium

ARTICLE INFO

Article history:

Received 3 September 2013

Accepted 18 November 2013

Available online 30 December 2013

Keywords:

$\text{Mg}(\text{BH}_4)_2$

Hydrogen desorption under dynamic vacuum

Torsion effusion vapor pressure measurements

Vaporization thermodynamics

ABSTRACT

The vapor pressure and molecular weight of effusing vapors of α , β , and amorphous $\text{Mg}(\text{BH}_4)_2$ were determined by Torsion-effusion gravimetric method, under dynamic vacuum. A Cahn balance in the system yielded the rate of the weight loss. Molecular weights measured revealed if the effusion was congruent or there was disproportionation. The vaporization behavior of crystalline $\text{Mg}(\text{BH}_4)_2$, was measured up to 533 K at pressures of $\sim 10^{-5}$ torr. It was found that $\text{Mg}(\text{BH}_4)_2$ disproportionates to form predominantly H_2 gas ($\sim 95\%$) with a small amount of $\text{Mg}(\text{BH}_4)_2$ ($\sim 5\%$) in the gas phase. The combined average molecular weight measured is 4.16 g/mol. The equations for vapor pressures for crystalline $\text{Mg}(\text{BH}_4)_2$ are given by: $\log P_{\text{Total}} (\text{bar}) = 9.2303 - 7286.2/T$, $\log P_{\text{Mg}(\text{BH}_4)_2} (\text{bar}) = 8.2515 - 7286.2/T$, and $\log P_{\text{H}_2} (\text{bar}) = 9.1821 - 7286.2/T$. The partial pressures of the gaseous species were determined as $P_{\text{Mg}(\text{BH}_4)_2(\text{g})}/P_T = 0.105$ and $P_{\text{H}_2(\text{g})}/P_T = 0.895$. Enthalpies of vaporization for the effusing gases were calculated to be $\Delta H = +558.0$ kJ/mol H_2 and $\Delta H = +135$ kJ/mol $\text{Mg}(\text{BH}_4)_2$. The standard Gibbs free energy changes, ΔG° (kJ/mol), for the complete decomposition reaction ($\text{Mg}(\text{BH}_4)_2(\text{s}) \rightarrow \text{Mg}(\text{s}) + 2\text{B}(\text{s}) + 4\text{H}_2(\text{g})$), sublimation reaction ($\text{Mg}(\text{BH}_4)_2(\text{s}) \rightarrow \text{Mg}(\text{BH}_4)_2(\text{g})$) and the disproportionation reaction for $\text{Mg}(\text{BH}_4)_2$ are reported in this paper. The decomposition pathway of amorphous $\text{Mg}(\text{BH}_4)_2$ was also carried out between 388.2 K and 712.8 K showing multistep decomposition of a- $\text{Mg}(\text{BH}_4)_2$. Different reaction products were obtained depending on the method used in the vaporization experiment. The behavior of the amorphous $\text{Mg}(\text{BH}_4)_2(\text{s})$ is very different from those for the two crystalline phases (α and β). The vapor pressure behavior and thermodynamics of vaporization of different phases of $\text{Mg}(\text{BH}_4)_2$ are presented.

Copyright © 2013, Hydrogen Energy Publications, LLC. Published by Elsevier Ltd. All rights reserved.

* Corresponding author. Tel.: +1 775 784 4960.

E-mail addresses: dchandra@unr.edu, chandra12321@yahoo.com (D. Chandra).

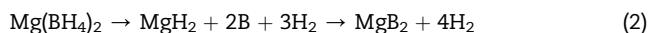
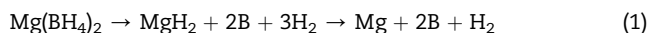
1. Introduction

The $\text{Mg}(\text{BH}_4)_2$ with 14.8 wt.% H storage capacity [1] makes it a material of interest for hydrogen storage. Many investigations have been made that show ~ 13.7 wt.% of hydrogen is released when $\text{Mg}(\text{BH}_4)_2$ is heated up to 870 K [2–15,28]. Several crystal structures have been proposed from theoretical and experimental studies of $\text{Mg}(\text{BH}_4)_2$. Konoplev and Bakulina [2] suggested the existence of two crystalline phases, the α -phase (claimed tetragonal) which is stable at room temperature up to ~ 180 °C when it transforms into the β -phase (claimed cubic face-centered). In other experimental work Riktor et al. [5] showed from *in situ* diffraction studies that there was a transition from the α - \rightarrow β -phase between 453 and 463 K, the β -phase decomposing above 518 K. Černý et al. [6] solved the structure of solvent-free α - $\text{Mg}(\text{BH}_4)_2$ from synchrotron X-ray and neutron diffraction experiments to be hexagonal with space group $P6_1$. Her et al. [7] also determined the α - $\text{Mg}(\text{BH}_4)_2$ in the hexagonal space group $P6_1$ using synchrotron X-ray alone. They also showed that the β -phase has an orthorhombic structure with space group $Fddd$. A structure revision for the α -phase to the $P6_122$ space group was proposed from DFT-optimization of the experimental structure by Dai et al. [now 8] and later confirmed by Filinchuk et al. [9] from single crystal synchrotron X-ray diffraction. The latter also noted that the α -phase contains small pores and at 490 K transforms irreversibly to the non-porous β -phase with $\sim 3\%$ higher density. At high pressures a new phase was observed by George et al. [10], and its crystal structure has been determined by Filinchuk et al. [11]. The high-pressure δ -phase can be quenched to ambient conditions, and features a double interpenetrated framework structure with nearly twice higher density than for the porous phase, known as γ - $\text{Mg}(\text{BH}_4)_2$ [11]. Remarkably, the porous phase is able to adsorb reversibly guest species, much like MOFs, and is considered the first porous hydride.

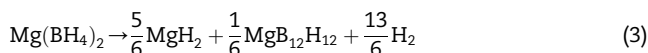
A lot of theoretical work has been done in an attempt to predict crystal structures of $\text{Mg}(\text{BH}_4)_2$ [8,11–20]. Nakamori et al. [12] suggested from first principle calculations the trigonal and monoclinic phases with the trigonal structure being the most stable. Vajeeston et al. [13] predicted a ground-state lowest energy $\text{Cd}(\text{AlCl}_4)_2$ -type monoclinic structure for $\text{Mg}(\text{BH}_4)_2$ with a higher symmetry orthorhombic space group $Pmc2_1$. First principles DFT calculations (at $T = 0$ K) by Ozolins et al. [14] predicted the crystal structure of $\text{Mg}(\text{BH}_4)_2$ to have symmetry of $I-4m2$ symmetry; 5 kJ/mol lower in energy than the previously experimentally determined structure with hexagonal $P6_1$ symmetry. van Setten et al. [15] determined a crystal structure for $\text{Mg}(\text{BH}_4)_2$ 17.6 kJ/mol lower in energy than the $Pmc2_1$ structure (generally used for calculating the $\text{Mg}(\text{BH}_4)_2$ structure). Voss et al. [16] reported a new $F222$ structure for $\text{Mg}(\text{BH}_4)_2$ from the $I-4m2$ phase of $\text{Mg}(\text{BH}_4)_2$ with a lower energy than all previously determined structures of $\text{Mg}(\text{BH}_4)_2$. Li et al. [17] predicted from first principle calculations that $\text{Mg}(\text{BH}_4)_2$ has a monoclinic structure with space group $P2_1/c$ (NO. 14). van Setten et al. [18] showed from DFT calculations of different stoichiometries of $\text{Mg}(\text{BH}_4)_2$ that most stable structures contained Mg^{2+} and $(\text{B}_2\text{H}_6)^{2-}$ ions. Caputo et al. [19] determined a ground state crystal structure of $\text{Mg}(\text{BH}_4)_2$ to be $I-4m2$. Zhou et al. [20] have obtained two ground state crystal structures for $\text{Mg}(\text{BH}_4)_2$, $I4_122$ and $F222$, lower in energy than the

previously determined $I-4m2$ phase. Remarkably, none of the experimentally determined structures known so far were predicted before the experimental structures were published and all the theoretically most stable $\text{Mg}(\text{BH}_4)_2$ structures are not yet observed. Interestingly, out of all the possible eight vertex MgH_8 polyhedra, only the less uniform Johnson solids are found in the experimental structures, while the theoretically predicted structures always contain MgH_8 cubes (see Table S6 in [Ref. 21]).

Several theoretical and experimental thermodynamic studies have been performed to determine the hydrogen desorption pathway of $\text{Mg}(\text{BH}_4)_2$. Early work by Konoplev and Bakulina [2] showed that the $\text{Mg}(\text{BH}_4)_2$ decomposed via a 2-step process: In the first step $\text{Mg}(\text{BH}_4)_2$ decomposes to MgH_2 with the evolution of hydrogen subsequently decomposes to Mg and B accompanied by additional hydrogen release [2]. Several other researchers have also proposed the decomposition of $\text{Mg}(\text{BH}_4)_2 \rightarrow \text{MgH}_2$ then to Mg and/or magnesium borides [3,10,12,21–23]. Thermal desorption profiles of $\text{Mg}(\text{BH}_4)_2$ by Nakamori et al. [12] suggest a multistep decomposition through intermediate hydrides and/or borides; these follow either Equation (1) or Equation (2):

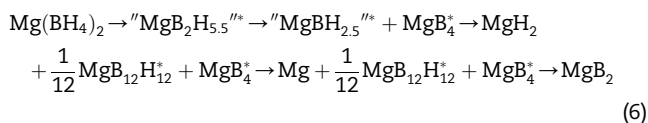


More recently, $\text{Mg}(\text{BH}_4)_2$ has been found to thermally desorb hydrogen by forming more complex intermediate compounds in a multi-step process. Chlopek et al. [3], based on simultaneous TGA, DSC and MS show that the thermal decomposition of $\text{Mg}(\text{BH}_4)_2$ proceeds via Equation (4) or more endothermic steps with Mg, MgB_2 and MgB_4 found as decomposition products. Li et al. [17,24,25] had initially proposed from their TG and PCT measurements, as well as theoretical studies show that $\text{MgB}_{12}\text{H}_{12}$ was a possible intermediate product in the multistep decomposition of $\text{Mg}(\text{BH}_4)_2$ as shown in the equations below:



Hwang et al. [26] confirmed the presence of $\text{MgB}_{12}\text{H}_{12}$, via ^{11}B NMR studies. First principle calculations by Ozolins et al. [14,27] show that decomposition of $\text{Mg}(\text{BH}_4)_2$ via $\text{MgB}_{12}\text{H}_{12}$ is the favored pathway in terms of equilibrium temperature at a H_2 pressure of 1 atm ($T_c = 293$ K) and H_2 desorption enthalpy at 298 K ($\Delta H = 29.5$ kJ/mol H_2), compared to $T_c = 348$ K, $\Delta H = 38.8$ kJ/mol H_2 for $\text{Mg}(\text{BH}_4)_2 \rightarrow \text{MgB}_2 + 4\text{H}_2$ and $T_c = 443$ K, $\Delta H = 47.3$ kJ/mol H_2 for $\text{Mg}(\text{BH}_4)_2 \rightarrow \text{MgH}_2 + \text{B} + 3\text{H}_2$, respectively. TG-DTA-DSC experiments by Hanada et al. [28] indicate that several hydrogen containing and amorphous boron containing compounds appear as intermediates in the several-steps thermal decomposition of $\text{Mg}(\text{BH}_4)_2$ to $\text{MgB}_2 + \text{H}_2$. DSC measurements by Yan et al. [29] also showed a multi-step decomposition reaction for $\text{Mg}(\text{BH}_4)_2$ going through $\text{MgB}_{12}\text{H}_{12}$. Soloveichik et al. [30] determined from results of TPD, DSC, *in situ* XRD, ^{11}B -NMR and a consideration of the amount of hydrogen produced at

each reaction step that crystalline $\text{Mg}(\text{BH}_4)_2$ decomposes via at least 4 steps with the formation of intermediate polyborane compounds such as $\text{MgB}_{12}\text{H}_{12}$. The major intermediates of this process, the amorphous phases denoted by asterisks, are shown in the reactions below:



The presence of an MgB_2H_6 species was shown from DFT calculations by van Setten et al. [18]. Severa et al. [31] noted that a possible side product of hydriding MgB_2 is $\text{MgB}_{12}\text{H}_{12}$. Newhouse et al. [32] have also detected the presence of amorphous $\text{Mg}(\text{B}_x\text{H}_y)_n$ intermediates which could include species containing $[\text{B}_{12}\text{H}_{12}]^{2-}$. Hence the prediction from calculations of the formation of $\text{MgB}_{12}\text{H}_{12}$ matches with experimental observations. Kim et al. [33] predicted from first principle calculations that $\text{Mg}(\text{BH}_4)_2$ decomposed according to Equation (3), the $\text{MgB}_{12}\text{H}_{12}$ formed becomes unstable in the presence of MgH_2 and decomposes at 520 K to MgB_2 . Kulkarni et al. [34] have predicted from first principles calculations that the amorphous phases, $\text{MgB}_{12}\text{H}_{12}$ and $\text{CaB}_{12}\text{H}_{12}$ observed experimentally during the decomposition of $\text{Mg}(\text{BH}_4)_2$ and $\text{Ca}(\text{BH}_4)_2$ are actually a mixture of a very large number of structurally distinct compounds which are very close in energy. Li et al. [35] predicted the possible existence of more than one intermediate phase in addition to $\text{MgB}_{12}\text{H}_{12}$ using DFT first principles cluster calculations. Very recently, Chong et al. [36] showed from a combination of PCT, TGA/MS and NMR spectroscopy that the first species formed in the dehydrogenation of $\text{Mg}(\text{BH}_4)_2$ at 473 K is magnesium triborane, $\text{Mg}(\text{B}_3\text{H}_8)_2$, meanwhile a complex mixture of polyborane species is formed via a condensation mechanism involving simultaneous B–H bond insertion and formation of H_2 and metal hydride at >573 K. Zhang et al. [37] confirmed the formation of amorphous $\text{Mg}(\text{B}_x\text{H}_y)_n$ species from their TEM, Raman spectra and TPD measurements. On the higher temperature end, it has been determined from the experiment and calculations that $\text{Mg}(\text{BH}_4)_2$ starts decomposing in the range 500–613 K [21,22,24,25,28–30,38]. Lower decomposition temperatures for $\text{Mg}(\text{BH}_4)_2$ have also been obtained. Voss et al. [16] found from theory that $\text{Mg}(\text{BH}_4)_2$ decomposes in the range of 400–470 K. Hagemann et al. [39] showed from deuterium–hydrogen exchange studies that it is possible for break the B–H bond in $\text{Mg}(\text{BH}_4)_2$ at temperatures as low as 405 K. Ozolins et al. [14] reported that $\text{Mg}(\text{BH}_4)_2$ decomposes to MgB_2 at 348 K [28], and at 293 K to $\text{MgB}_{12}\text{H}_{12}$. van Setten et al. [18] showed that $\text{Mg}(\text{BH}_4)_2$ desorbs at 344 K to MgB_2 . Notably, DFT calculations by Kim et al. [36] show that $\text{Mg}(\text{BH}_4)_2$ decomposes slightly above RT (300 K) according to the Equation (3).

The measured dehydrogenation enthalpies for $\text{Mg}(\text{BH}_4)_2$ varied significantly in the literature, 67 ± 7 kJ/mol $\text{Mg}(\text{BH}_4)_2$ from DSC measurements by Chlopek et al. [3]; 38 kJ/mol H_2 (RT) from DFT calculations for $\alpha\text{-Mg}(\text{BH}_4)_2 \rightarrow \text{MgB}_2 + 4\text{H}_2$ and 51 kJ/mol H_2 (RT) for $\text{Mg}(\text{BH}_4)_2 \rightarrow \text{Mg} + 2\text{B} + 4\text{H}_2$ by van Setten et al. [18] 39.3 kJ/mol H_2 for $\text{Mg}(\text{BH}_4)_2 \rightarrow \text{MgH}_2 + \text{B} + 3\text{H}_2$ from experiment [21]; 57 ± 5 kJ/mol H_2 based on PCT measurements for $\text{Mg}(\text{BH}_4)_2 \rightarrow \text{MgH}_2 + \text{B} + 3\text{H}_2$ by Li et al. [17]. Ozolins et al. [14] calculated $\Delta H_{\text{Eq. 3}}$ (298 K) to be 29.5 kJ/mol H_2 , 38.8 kJ/mol H_2 for

reaction products $\text{MgB}_2 + 4\text{H}_2$ and 47.3 kJ/mol H_2 for $\text{MgH}_2 + \text{B} + 3\text{H}_2$, and in a subsequent paper [27] determined ΔH (300 K) = 50.0 kJ/mol H_2 for $\text{MgB}_{12}\text{H}_{12} + 5\text{MgH}_2 \rightarrow 6\text{MgB}_2 + 11\text{H}_2$; Yan et al. [29] have reported desorption enthalpies from DSC measurements of 44 ± 3 kJ/mol H_2 , 40 ± 2 kJ/mol H_2 and 38 kJ/mol H_2 for Reactions (3)+(4); 43 ± 3 kJ/mol H_2 , 40 ± 2 kJ/mol H_2 , 39 ± 2 kJ/mol H_2 , for Reactions (3)+(4)+(5); $46.9\text{--}50.3$ kJ/mol H_2 for Equation (3). Kulkarni et al. [34] determined 58.3–59.9 kJ/mol H_2 for $\text{MgB}_{12}\text{H}_{12} + 5\text{MgH}_2 \rightarrow 6\text{MgB}_2 + 11\text{H}_2$ by. This difference in values, as other researchers have noted, is most probably due to a difference in the method of measurement, both experimental and theoretical.

In this paper, we present a study of the vaporization behavior and desorption pathways of pure $\text{Mg}(\text{BH}_4)_2$ using the torsion-effusion gravimetric method. It should be noted that these studies are performed under dynamic vacuum. Three different types of samples were used: (1) crystalline $\alpha\text{-Mg}(\text{BH}_4)_2$, (2) crystalline $\beta\text{-Mg}(\text{BH}_4)_2$ with a catalyst, (3) amorphous $\text{Mg}(\text{BH}_4)_2$. The total vapor pressures at each stage of decomposition, as well as the average molecular weights of vapor species were obtained by gravimetric analysis of the effusing vapors. The reaction pathways for decomposition are shown. Standard enthalpies of formation and other thermodynamic properties of $\text{Mg}(\text{BH}_4)_2$ were obtained from a second law analyses of the decomposition process.

2. Experimental and calculations

2.1. Starting materials and instrumentation

Three vaporization experiments of $\text{Mg}(\text{BH}_4)_2$ were carried out. The first $\text{Mg}(\text{BH}_4)_2$ sample was from MHCoe Partner, General Electric, second sample was from the University of Geneva, Switzerland and the third amorphous sample was obtained from Aldrich Chemical Co. The second sample was prepared via a slight modification of Chlopek et al.'s method [3] and analyzed by X-ray powder diffraction. An appropriate amount of MgH_2 was ball milled for 2 h. Et_3NBH_3 was added to this ball milled powder, the mixture heated to 373 K for 1 h, then left to cool with overnight stirring [39]. The resulting solution was heated to 418 K for 6 h then cooled down. 180 ml of cyclohexane were added and the solution stirred for 2 days [39]. The light gray powder obtained was filtered and dried overnight under vacuum at room temperature. This light gray powder is again heated under vacuum up to 443 K to remove solvated Et_3N [39]. The $\alpha\text{-Mg}(\text{BH}_4)_2$ powder obtained was >95% pure as indicated on the X-ray powder diffraction profile taken at Laboratory X-ray diffractometer at the University of Geneva ($\text{CuK}\alpha 1$ radiation). X-ray diffraction powder analyses for other samples were performed at the University of Nevada, Reno using a PANalytical X'Pert PRO (PW3040-PRO) machine with $\text{Cu-K}\alpha$ radiation. A TG analysis of the starting $\text{Mg}(\text{BH}_4)_2$ material was done at the University of Geneva. All other TGA analyses were done using a TGA Q500 machine. A DSC Q100 V9.0 Build 275 (Universal V4.1D TA Instruments) machine was used to analyze the decomposition profile of the starting $\text{Mg}(\text{BH}_4)_2$ material. Laboratory X-ray diffraction powder analyses were performed using a PANalytical X'Pert PRO (PW3040-PRO) machine with $\text{Cu-K}\alpha$ radiation. The TGA analyses were done using a TGA

Q500 machine. A DSC Q100 V9.0 Build 275 (Universal V4.1D TA Instruments) machine was used to analyze the decomposition profile of the starting $\text{Mg}(\text{BH}_4)_2$ material.

2.2. The torsion-effusion apparatus

J. Margrave [40] described the general methodology for the measurement of vapor pressures. A torsion effusion thermogravimetric apparatus at the University of Nevada, Reno was used to measure the vaporization thermodynamics of $\text{Mg}(\text{BH}_4)_2$ [41,42]. The instrument is composed of two main assemblies: (1) the torsion-effusion component which measures the vapor pressure from angular displacement, and (2) the gravimetric component which is used to measure the average molecular weight of the effusing vapors. The torsion-effusion component is made up of the sample container which is a double-chamber molybdenum Knudsen cell with orifices in opposing directions in order to develop a moment when the effusing vapors are generated. This Knudsen cell pair is suspended by a thin fiber of approximately 58.6 cm long on one side of a Cahn Digital recording balance (Model D-100) [41,42]. The fiber is attached to a mirror assembly on a damping disc. The fiber-Knudsen cell assembly is encased in a quartz tube of $\sim 3.5''$ in diameter. The ribbon's fiber constant used in this instrument is 0.0674 dyne cm/rad. The vapor pressure data for $\text{Mg}(\text{BH}_4)_2$ was obtained using a 0.6 mm cell. Typical pressures attained in the instrument are of the order of 10^{-5} to 10^{-7} torr, afforded by a Turbo vacuum pump [41,42]. A sample of ~ 0.5 g is loaded into molybdenum Knudsen cells in a MBraun Labmaster 130 glove box filled with Ar, then transferred to the torsion-effusion instrument. The torsion effusion apparatus has a temperature capability of -293 K to 873 – 973 K. The $\text{Mg}(\text{BH}_4)_2$ samples were loaded into each of the Knudsen cells at room temperature. The sample is slowly heated up to the point where an angular deflection could be recorded [41–46].

The average molecular weights of the effusing vapors were also determined from weight loss plots that accompanied the effusion process. The molecular flux of gases can be determined according to the methods outlined in references [37–43]. The total vapor pressure, P_T , of the effusing gas was obtained from the Equation (7) [40,43,44]:

$$P_T = |K2\theta| / \left[\sum_{i=1}^n (a_i f_i d_i) \right] \quad (7)$$

where K is the fiber torsion constant, θ is the measured angular deflection, d_i is the moment arm of the effusion orifice, a_i is the area of the orifice, f_i is the force factor through the orifice i , and i is the number of Knudsen cell chambers [37–43], which is two in our case. The effusing gases accompanied by weight loss of the original sample cause angular deflection of the Knudsen cell and mirror used in the torsion effusion system. This angular deflection value together with the determination of the rate of weight loss in the sample is used to obtain the average molecular weights (M) of the effusing species using the formula [40,43,44]:

$$M = 2\pi RT \left[W \frac{\sum_{i=1}^n (a_i f_i d_i)}{(K2\theta) \sum_{i=1}^n (C \cdot a_i)} \right]^2 \quad (8)$$

where, R is the universal gas constant, T is the absolute temperature, W is the total rate of weight loss, a is the cross-sectional area of the orifice, and C is the Clausing factor of the orifice. Equation (9) below is used to calculate the average of molecular weights, M , for a system where more than one species is effusing at the same time:

$$M = \left(\sum_{i=1}^N m_i M_i^{-1/2} \right)^{-2} \quad (9)$$

where, N is the total number of species effusing from the sample, M_i is the molecular weight of species i , and m_i is the mass fraction of species i .

The torsion effusion instrument was calibrated for accuracy by measuring the vapor pressure of KCl. It was compared to the standard vapor pressure of KCl and was found to have a high absolute accuracy [40].

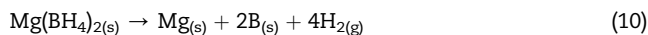
3. Results and discussion

3.1. Vaporization between 498 K and 533 K using β - $\text{Mg}(\text{BH}_4)_2$

The first set of experiments was performed using β - $\text{Mg}(\text{BH}_4)_2$. The vaporization results of $\text{Mg}(\text{BH}_4)_2$ in the temperature range of 498 K–533 K are listed in Table 1 and plotted in Fig. 1. Concurrent thermogravimetry yielded rate of weight loss during these vapor pressure also shown in Table 1. The average molecular weight determined from this experiment is 2.42 g/mol. This implies that the vapor phase is predominantly hydrogen. Thus $\text{Mg}(\text{BH}_4)_2$ was found to disproportionate at temperatures < 536 K. Complete vigorous decomposition of $\text{Mg}(\text{BH}_4)_2$ may occur at $T > 548$ K resulting in the decomposition of $\text{Mg}(\text{BH}_4)_2$; the experiment was stopped due to vigorous gas release above 548 K.

X-ray diffraction pattern of the starting material, β - $\text{Mg}(\text{BH}_4)_2$, is shown in Fig. 2(a) and (b) after the heating to > 548 K (at the end of the experiment). The XRD pattern in Fig. 2(a) matches β - $\text{Mg}(\text{BH}_4)_2$ pattern that has been reported by several investigators [3,4,24,25,31].

We propose from the results of X-ray diffraction that $\text{Mg}(\text{BH}_4)_2$ completely decomposes into solid Mg and H_2 gas according to the equation:



The residue from the vaporization experiment was dark brown in color suggesting the presence of amorphous boron. The XRD pattern of the residual powder (dark brown) shows

Table 1 – Total Pressures (P_T) of effusing vapors for the disproportionation of $\text{Mg}(\text{BH}_4)_{2(s)} \rightarrow 0.018\text{Mg}(\text{BH}_4)_{2(g)} + 0.982\text{H}_{2(g)}$ measured by torsion-effusion gravimetric method using a 0.3 mm Mo Knudsen cells.

T, K	P_T , bar	Wt. loss, mg/h	MW, g/mol
498.15	8.92×10^{-6}	–	–
508.15	9.36×10^{-6}	0.161	2.22
518.15	1.16×10^{-5}	0.180	1.85
523.15	1.69×10^{-5}	0.368	3.66
528.15	2.67×10^{-5}	0.422	1.95
533.15	3.31×10^{-5}	–	–

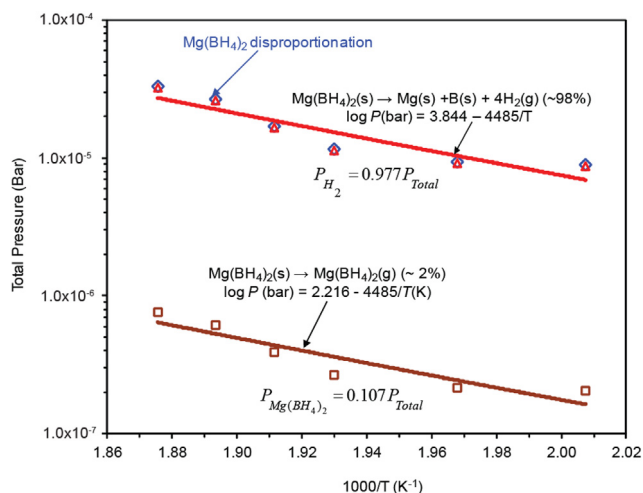


Fig. 1 – Vapor pressures of $\text{Mg}(\text{BH}_4)_2$ and H_2 represented by the reactions $\text{Mg}(\text{BH}_4)_2(\text{s}) \rightarrow \text{Mg}(\text{BH}_4)_2(\text{g})$ and $\text{Mg}(\text{BH}_4)_2(\text{s}) \rightarrow \text{Mg}(\text{s}) + 2\text{B}(\text{s}) + 4\text{H}_2(\text{g})$ obtained using a Mo Knudsen cell with orifice diameter of 0.3 mm.

evidence of pure magnesium (Fig. 2). Although elemental boron or MgB_2 was not detected by XRD, it was suspected that boron exists in amorphous phase.

The measured molecular weight of the effusing vapors obtained from the vaporization experiment is 2.42 g/mol; this is slightly higher than that of molecular hydrogen (2.016 g/mol), but it is far lower than that of pure $\text{Mg}(\text{BH}_4)_2$ (53.99 g/mol); a small amount of $\text{Mg}(\text{BH}_4)_2$ exists in the vapor phase just above the solid. Ideally, congruent vaporization of $\text{Mg}(\text{BH}_4)_2$ should be according to the equation:



However, in this study, the proposed vaporization behavior of $\text{Mg}(\text{BH}_4)_2$ can be represented as the disproportionation Equation (12):

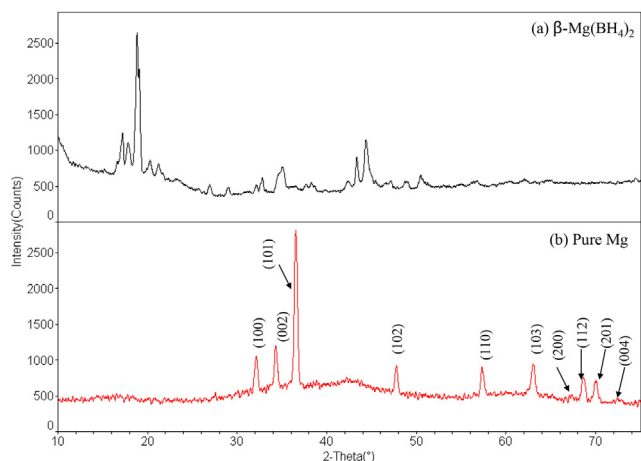
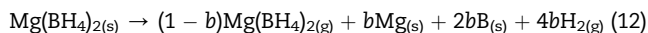
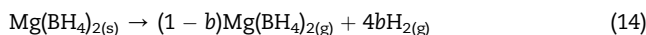


Fig. 2 – Powder X-ray diffraction pattern of $\text{Mg}(\text{BH}_4)_2$ MHCoe Partner, General Electric (a) $\beta\text{-Mg}(\text{BH}_4)_2$ and (b) metallic Mg obtained in the residue obtained after heating up to 548 K.

where b is the fraction of solid $\text{Mg}(\text{BH}_4)_2$ that disproportionates. These data are plotted as $\log P_T$ (bar) versus $1/T$, (Fig. 1) to obtain the vapor pressure equation:

$$\log P_T \text{ (bar)} = +3.8539 - 4485/T \quad (13)$$

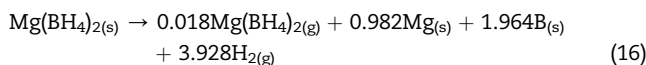
The general disproportionation reaction of $\text{Mg}(\text{BH}_4)_2$ can be re-written taking into consideration only the effusing vapors which contribute to the vapor pressure of $\text{Mg}(\text{BH}_4)_2$ as:



The molecular weights of the effusing species were obtained by the derived Equation (15) given below:

$$M = \left(\sum_{i=1}^N m_i M_i^{-1/2} \right)^{-2} = \left[\frac{[(1-b)M_{\text{Mg}(\text{BH}_4)_2(\text{g})}^{1/2} + 4bM_{\text{H}_2(\text{g})}^{1/2}]}{[(1-b)M_{\text{Mg}(\text{BH}_4)_2(\text{g})} + 4bM_{\text{H}_2(\text{g})}]} \right]^{-2} \quad (15)$$

In order to find the value of ' b ' that shows the fraction of the effusing gas disproportionated to hydrogen gas, we use the Equation (15); in this, the measured value of $M = 2.42$ g/mol, and the known molecular weights for pure $M_{\text{Mg}(\text{BH}_4)_2(\text{g})}$ and M_{H_2} gases are substituted (on the right hand side) in the Equation (15). Thus a general equation for $b = -0.7433 \log M + 1.437$. The corresponding value of b for the measured molecular weight, $M = 2.42$ g/mol is 0.982, and $(1-b) = 0.018$. Substituting $b = 0.982$ into the proposed complete disproportionation Equation (12) gives:



The partial pressures of the gases which constitute the effusing vapors can be determined from which the individual decomposition equations can be obtained as well as the Gibbs free energies and other thermodynamic constants. The partial pressure of $\text{Mg}(\text{BH}_4)_2$ may be expressed as:

$$\frac{P_{\text{Mg}(\text{BH}_4)_2(\text{g})}}{P_T} = \left[\frac{(1-b)M_{\text{Mg}(\text{BH}_4)_2(\text{g})}^{1/2}}{(1-b)M_{\text{Mg}(\text{BH}_4)_2(\text{g})}^{1/2} + 4bM_{\text{H}_2(\text{g})}^{1/2}} \right]^{-2} \quad (17)$$

and the partial pressure of H_2 can be represented as:

$$\frac{P_{\text{H}_2}}{P_T} = \left[\frac{4bM_{\text{H}_2(\text{g})}^{1/2}}{(1-b)M_{\text{Mg}(\text{BH}_4)_2(\text{g})}^{1/2} + 4bM_{\text{H}_2(\text{g})}^{1/2}} \right]^{-2} \quad (18)$$

When b is substituted into Equations (17) and (18), partial pressures of $\text{Mg}(\text{BH}_4)_2(\text{g})$ and $\text{H}_2(\text{g})$ are obtained as:

$$\begin{aligned} \frac{P_{\text{Mg}(\text{BH}_4)_2(\text{g})}}{P_T} &= 0.023 \text{ or } \log P_{\text{Mg}(\text{BH}_4)_2(\text{g})} = \log 0.023 + \log P_T \\ &= 2.216 - 4485/T \end{aligned} \quad (19)$$

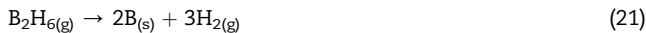
$$\begin{aligned} \frac{P_{\text{H}_2(\text{g})}}{P_T} &= 0.977 \text{ or } \log P_{\text{H}_2(\text{g})} = \log 0.977 + \log P_T = 3.844 - 4485/T \end{aligned} \quad (20)$$

The P_{Total} , $P_{\text{Mg}(\text{BH}_4)_2}$ (~2%), and P_{H_2} (~98%) plots are shown in Fig. 1. Approximately 98% of the total pressure is due to hydrogen evolution. The partial pressures of $\text{Mg}(\text{BH}_4)_2(\text{g}) = 4.37 \times 10^{-5}$ bar and 1.87×10^{-5} bar $\text{H}_2(\text{g})$ at 523 K.

We compare vapor pressure of MgH_2 and Mg with vapor pressures of the decomposed $\text{Mg}(\text{BH}_4)_2$ in Fig. 3. It can be seen

that the $\text{Mg}(\text{BH}_4)_2$ vapor pressures are higher as compared to Mg ($\text{Mg}_{(s)} \rightarrow \text{Mg}_{(g)}$), but are lower than for MgH_2 vapor pressure ($\text{MgH}_{2(s)} \rightarrow \text{Mg}_{(s)} + \text{H}_{2(g)}$), from literature [47,48] observed from 498 K to 533 K.

The possibility of forming other gaseous species such as BH_3 , B_2H_6 (27.67 g/mol), has been considered. Equations (21) and (22) show two ways by which diborane could decompose after formation. The more feasible reaction is Equation (21) where diborane decomposes to form solid B and H_2 gas.



At 298 K and 1 bar, $\Delta G_{\text{rxn}} = -87.6$ kJ/mol.



At 298 K and 1 bar, $\Delta G_{\text{rxn}} = +1042.4$ kJ/mol.

The vapor pressure experimental conditions were from 473 K–548 K and 10^{-4} – 10^{-5} torr. Due to exothermic nature of the decomposition as well as the increase in the number of moles of product, the decomposition of $\text{B}_2\text{H}_{6(g)}$ may not be favored and diborane may exist in the vapor phase. Thermolysis of diborane has been studied extensively and reaction mechanism is complex [49].

3.2. Vaporization of between 438 K and 489 K using α - $\text{Mg}(\text{BH}_4)_2$

Vapor pressure experiments were performed to study the vaporization behavior of α - $\text{Mg}(\text{BH}_4)_2$ in a lower temperature range of 438 K–489 K. The total vapor pressure data measured using a pair of 0.6 mm orifice molybdenum Knudsen cells is shown on Table 2 and these data are plotted in Fig. 4. The molecular weights of the effusing vapors were only obtained at above 488 K. This is probably due to poor kinetics at lower temperatures than 488 K. The pressure equation obtained using the second law and the slope of the line is:

$$\log P_T \text{ (bar)} = +8.8629 - 7123.8/T \quad (23)$$

Initial TG (at Setaram Inc., Newark, CA) and DSC analysis of the hydrogen desorption process and thermal stability of the

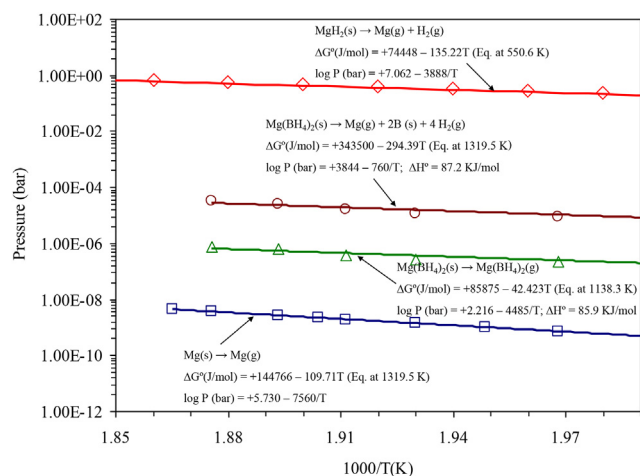


Fig. 3 – Vaporization behavior of Mg [44] and MgH_2 [45] from literature compared to the vaporization of $\text{Mg}(\text{BH}_4)_2$ observed from 498 K to 533 K using the torsion effusion method.

as-received α - $\text{Mg}(\text{BH}_4)_2$ was done. The combined results of the TG and DSC results obtained are shown in Fig. 5.

It can be clearly seen on the TG plot that the slope of the TG curve (Fig. 5(a)) starts changing at 412.6 K and keeps changing until the highest temperature is reached of 673 K. This same pattern of change in the slope of the TG curve for $\text{Mg}(\text{BH}_4)_2$ has been observed earlier [3,4,17,21–25,31]. The fact that the slope of the TG curve is changing indicates that the decomposition of α - $\text{Mg}(\text{BH}_4)_2$ proceeds via a multi-step reaction. The solid sample in the two Knudsen cells vaporizes between 5334 K and 673 K; gravimetric measurements show that mostly H_2 gas is evolved in this temperature range. Complementary DSC analyses show several endothermic and one exothermic event (Fig. 5(b)) [3,4,25,28–31]. The several endothermic processes indicate that the decomposition of $\text{Mg}(\text{BH}_4)_2$ indeed proceeds via several steps. The sample lost most weight in the temperature range of 472.97 K–477.76 K. The first peak at approximately 478 K (segment (A)) indicates the polymorphic transformation from the α phase to the β phase of $\text{Mg}(\text{BH}_4)_2$ [2,3,6,12,28,30].

The TG curve confirms that there is no loss in mass of the sample [2,3] up to approximately 573 K. The two main decomposition endothermic peaks at 581.84 K and 651.39 K (segments (B) and (E)) can be attributed to the decomposition of $\text{Mg}(\text{BH}_4)_2$ [2,23,30] to mainly MgH_2 [3,12,21–23,30], and decomposition of MgH_2 into elements [12,21–23,30]. The exothermic peak at approximately 620 K (segment (C)) has been attributed to amorphous MgH_2 becoming crystalline [2,23,30], but the presence of the wiggly sharp lines or shoulders just after the peak at 581.84 K (between 583 K and 593 K) strongly suggests that other less important intermediates could be present with amorphous MgH_2 and are decomposing at this temperature [5,21,24]. The endothermic event at ~ 639 K (segment (D)) is probably a major intermediate compound decomposing at a lower temperature than MgH_2 to form Mg or MgB_2 . This is likely to correspond to the formation of one of the more stable intermediates in the process of

Table 2 – Total pressures (P_T) of effusing vapors for the disproportionation reaction $\text{Mg}(\text{BH}_4)_{2(s)} \rightarrow (1-b)\text{Mg}(\text{BH}_4)_{2(s)} + 3b\text{H}_{2(g)}$ measured by torsion effusion method using 0.6 mm orifice diameter Mo Knudsen cells in the temperature range 438 K–489 K.

T, K	P_T , bar	Weight loss, mg/h	MW, g/mol
438.06	5.9592×10^{-8}	–	–
439.97	6.2729×10^{-8}	–	–
452.82	1.0664×10^{-7}	–	–
453.76	1.0978×10^{-7}	–	–
453.82	1.1919×10^{-7}	–	–
454.62	1.5683×10^{-7}	–	–
457.83	1.4115×10^{-7}	–	–
458.09	1.4115×10^{-7}	–	–
462.75	1.5056×10^{-7}	–	–
462.82	1.7879×10^{-7}	–	–
463.55	2.4466×10^{-7}	–	–
467.51	3.2935×10^{-7}	–	–
467.73	3.4817×10^{-7}	–	–
473.22	7.3693×10^{-7}	–	–
474.72	4.5167×10^{-7}	–	–
480.63	9.6551×10^{-7}	–	–
488.69	2.7527×10^{-6}	0.2488	7.50
488.91	2.3789×10^{-6}	0.2186	7.78

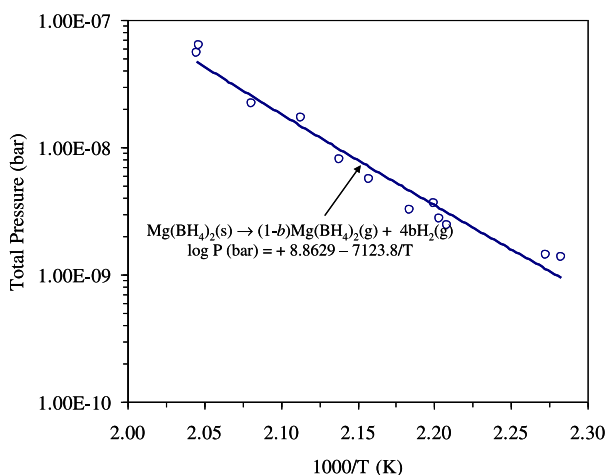


Fig. 4 – Vapor pressure measured for $\text{Mg}(\text{BH}_4)_2(\text{s}) \rightarrow (1 - b)\text{Mg}(\text{BH}_4)_2(\text{g}) + 4b\text{H}_2(\text{g})$ within the temperature range 438 K–489 K.

$\text{Mg}(\text{BH}_4)_2$ decomposition. The slope changes in the TG correspond to the transformations on the DSC (Fig. 5).

A second DSC experiment was carried out after torsion effusion vaporization of the α - $\text{Mg}(\text{BH}_4)_2$ sample up to 489 K at pressures of 10^{-5} torr. This DSC curve (Fig. 6(b)) is very similar to the one obtained before the experiment (Fig. 6(a)) suggesting that the sample is still mostly composed of $\text{Mg}(\text{BH}_4)_2$. It can be clearly seen on this plot that there is still some α - $\text{Mg}(\text{BH}_4)_2$ present even at temperatures up to 489 K. The endothermic event at ~ 477 K suggests the presence of some α - $\text{Mg}(\text{BH}_4)_2$ that transforms to β - $\text{Mg}(\text{BH}_4)_2$. By comparing relative intensities of the peaks in Fig. 6(b) compared to Fig. 6(a).

The XRD pattern of α - $\text{Mg}(\text{BH}_4)_2$ from the University of Geneva, used in this experiment is shown in Fig. 7, reveals only small amount of impurities. The data fit very well the reported crystal structure and the earlier published powder patterns [3,6,7,14,26,32,33,39]. The sample loaded (0.2071 g) into the torsion effusion instrument was white in color before

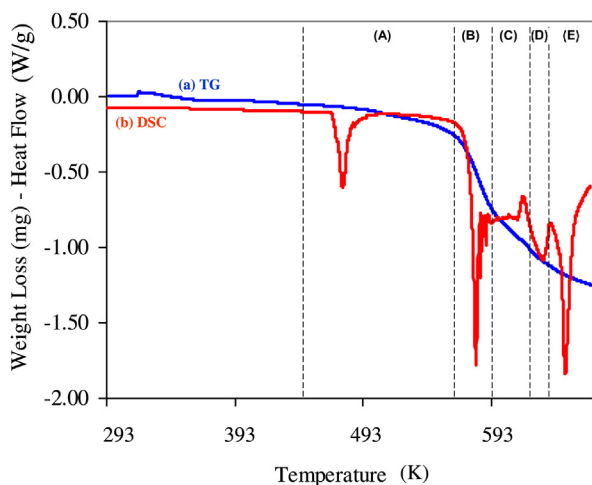


Fig. 5 – (a) TG and (b) DSC (done at a rate of 275 K/min under N_2 atmosphere) profiles of $\text{Mg}(\text{BH}_4)_2$ obtained from the University of Geneva, before vaporization.

the experiment was turned to off-white to very light gray in color after the experiment (0.0107 g); a 5.2 wt.% loss.

The XRD profile of the post vaporization sample (Fig. A-1 in Appendix) was identified as mostly β - $\text{Mg}(\text{BH}_4)_2$. We did not observe any MgH_2 , MgB_2 or Mg Bragg peaks. This pattern for β - $\text{Mg}(\text{BH}_4)_2$ is very similar to what has been reported [3–5,25] as well as to the pattern for the $\text{Mg}(\text{BH}_4)_2$ sample obtained from our GE collaborators (Fig. 2(b)).

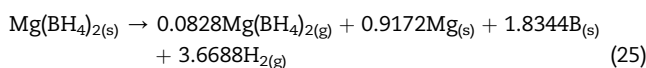
3.3. Summary of low and high temperature range vapor pressure results

As the residue from second vaporization experiment was β - $\text{Mg}(\text{BH}_4)_2$ and the first experiment was carried out with β - $\text{Mg}(\text{BH}_4)_2$, the vapor pressure results from the first set of experiments within 498–533 K and the second set of experiments between 438 K and 489 K were combined. The low and high temperature vapor pressure data are combined; these measurements were taken at different times (Fig. 8). The thermal decomposition and vaporization behavior of $\text{Mg}(\text{BH}_4)_2$ within the combined temperature range of 438 K–533 K is still well represented by the Equation (12). The total vapor pressure equation is given by:

$$\log P_T (\text{bar}) = 9.2303 - 7286.2/T \quad (24)$$

Equation (15) was used to determine the molecular weight for this combined data. The obtained value of 4.16 g/mol is closest to the molecular weight of H_2 compared to other products which could be present in the gaseous phase. A general equation for $b = -0.743 \log M + 1.436$ was obtained after substituting the molecular weight of pure $\text{Mg}(\text{BH}_4)_2$ and pure H_2 .

Substituting the measured molecular weight obtained of 4.16 g/mol, we get a b value of 0.9172. The vaporization behavior can therefore be represented as:



The partial pressures of $\text{Mg}(\text{BH}_4)_2$ and H_2 gases for this experiment can be obtained using Equations (26) and (27) to give:

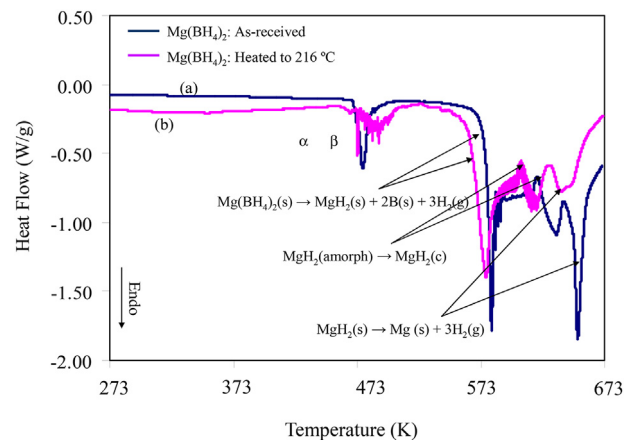


Fig. 6 – DSC analysis of $\text{Mg}(\text{BH}_4)_2$ powder from Geneva (a) before and (b) after heating to 489 K.

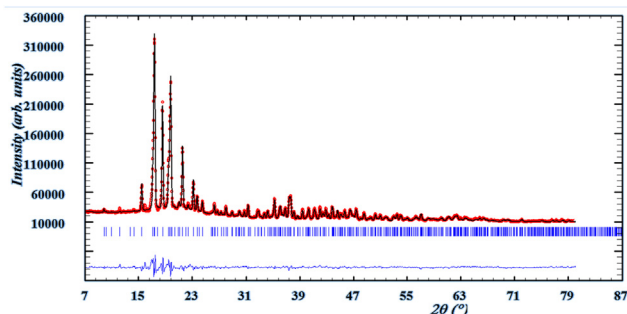


Fig. 7 – Rietveld X-ray powder diffraction profile of α - $\text{Mg}(\text{BH}_4)_2$ taken using monochromatic $\text{CuK}\alpha 1$ radiation.

$$\frac{P_{\text{Mg}(\text{BH}_4)_2(\text{g})}}{P_T} = 0.105 \text{ or } \log P_{\text{Mg}(\text{BH}_4)_2(\text{g})} = \log 0.105 + \log P_T$$

$$= 8.2515 - 7286.2/T \quad (26)$$

$$\frac{P_{\text{H}_2(\text{g})}}{P_T} = 0.895 \text{ or } \log P_{\text{H}_2(\text{g})} = \log 0.895 + \log P_T$$

$$= 9.1821 - 7286.2/T \quad (27)$$

The two reactions occurring here based on molecular weight value of effusing vapors are represented in Equations (10) and (11). The equation for the direct vaporization of $\text{Mg}(\text{BH}_4)_2$ in a solid–gas equilibrium can be written as Equation (11), for which

$$K_p = P_{\text{Mg}(\text{BH}_4)_2(\text{g})} = 0.105P_T \quad (28)$$

and

$$\Delta G^\circ_{\text{Mg}(\text{BH}_4)_2(\text{g})} (\text{J/mol}) = -RT \ln K_p = 139510 - 158T \quad (29)$$

From the second law of thermodynamics, $\Delta H_{\text{rxn}} = +139.5$ kJ/mol. Decomposition of $\text{Mg}(\text{BH}_4)_2$ also occurs simultaneously to H_2 and can be represented by the above Equation (10), for which

$$K_p = (P_{\text{H}_2(\text{g})})^4 = (0.895P_T)^4 \quad (30)$$

and

$$\Delta G^\circ_{\text{H}_2(\text{g})} (\text{J/mol}) = -RT \ln K_p = 558040 - 703.3T \quad (31)$$

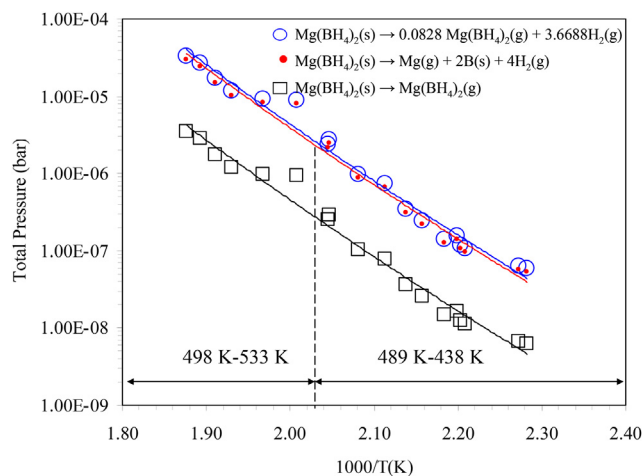


Fig. 8 – Partial pressures of $\text{Mg}(\text{BH}_4)_2$ and H_2 represented by the reactions $\text{Mg}(\text{BH}_4)_2(\text{s}) \rightarrow \text{Mg}(\text{BH}_4)_2(\text{g})$ and $\text{Mg}(\text{BH}_4)_2(\text{s}) \rightarrow \text{Mg}(\text{g}) + 2\text{B}(\text{s}) + 4\text{H}_2(\text{g})$ and total disproportionation pressure of $\text{Mg}(\text{BH}_4)_2$ from 438 K to 533 K.

From the second law of thermodynamics, $\Delta H_{\text{rxn}} = +558.0$ kJ/mol. The total Gibbs free energy change for the disproportionation Reaction (25) for which

$$K_p = \left[(0.105P_T)^{0.0828} \cdot (0.895P_T)^{3.6688} \right] \quad (32)$$

is given by:

$$\Delta G^\circ_{\text{subl.}} (\text{J/mol}) = -RT \ln K_p = 523385 - 658.1T \quad (33)$$

From the second law of thermodynamics, $\Delta H_{\text{rxn}} = +523.4$ kJ/mol.

The Gibbs free energy changes for the decomposition of $\text{Mg}(\text{BH}_4)_2$ (Equation (10)), sublimation of $\text{Mg}(\text{BH}_4)_2$ (Equation (11)) and disproportionation of $\text{Mg}(\text{BH}_4)_2$ (Equation (25)) are plotted in Fig. 9.

A complete vaporization analysis of $\text{Mg}(\text{BH}_4)_2$ from 388.2 K to 712.8 K and under moderate pressures of 10^{-5} torr was done using powder obtained from Aldrich using torsion effusion and gravimetry. The vapor pressure data obtained is shown on Table A-1 (see appendix). The XRD profile of the as-received starting material (white in color) showed that the sample was amorphous. Crystallization of these $\text{Mg}(\text{BH}_4)_2$ powders was attempted using a Sievert's apparatus by heating the material to 473 K under H_2 pressure for a day, then cooled down to RT and evacuated at RT to remove any extra H_2 that could be present. An XRD analysis of the powder after this procedure still turned out amorphous, so the material was characterized by DSC and in situ powder X-ray diffraction under vacuum at various temperatures, but both results still showed that the material was amorphous. 0.2522 g of this powder was loaded and the vaporization experiment was carried out according to the procedure outlined in the experimental.

The total vapor pressure data using a pair of 0.6 mm orifice Knudsen cells is plotted in Fig. 10. The presence of several plots in Fig. 10 is indicative of the presence of several intermediate compounds which are close together in energy and decompose to release hydrogen at similar energies. This also affirms the fact that the decomposition of $\text{Mg}(\text{BH}_4)_2$ is a very complicated process and can be linked to the complex structure of $\text{Mg}(\text{BH}_4)_2$ [11,14,19–30]. This observation could be linked to results

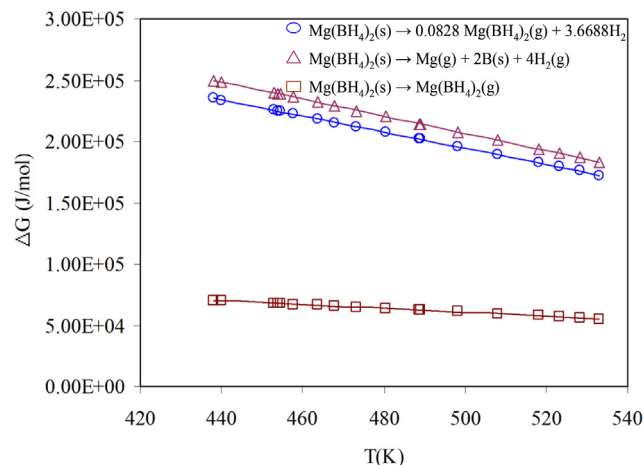


Fig. 9 – Gibbs free energy changes for sublimation (\square), decomposition (Δ) and disproportionation (\circ) reaction from 438 K to 533 K.

obtained from first principles DFT calculations Kulkarni et al. [34] from which they determined the existence of a multitude of compounds with different ground state structures having very similar energies. They also observed from first principles molecular dynamics calculations that it was possible to obtain near room temperature an X-ray diffraction pattern showing the presence of amorphous compounds [31].

Vapor pressure plots are obtained for temperatures as low as 388.2 K. This observation of vapor pressures at low temperatures is an achievement since there has been several reports from calculations as well as experiments on the possibility of the hydrogen desorption of $\text{Mg}(\text{BH}_4)_2$ at low temperatures. Voss et al. [16] found from theory that $\text{Mg}(\text{BH}_4)_2$ decomposes in the range of 400–470 K. Hagemann et al. [39] showed from deuterium–hydrogen exchange studies that it is possible for the B–H bond in $\text{Mg}(\text{BH}_4)_2$ to be broken at temperatures as low as 405 K. Ozolins et al. have shown from DFT calculations and from a thermodynamic standpoint that $\text{Mg}(\text{BH}_4)_2$ desorbs to MgB_2 at 348 K [27] and at 293 K to $\text{MgB}_{12}\text{H}_{12}$ [14]. van Setten et al. [18] showed that $\text{Mg}(\text{BH}_4)_2$ desorbs at 344 K to MgB_2 . Notably, DFT calculations by Kim et al. [33] show that $\text{Mg}(\text{BH}_4)_2$ decomposes slightly above RT (300 K) according to Equation (3).

The presence of several vapor pressure lines can also be attributed to the fact that different results can be obtained depending on the mechanism used to obtain the vapor pressures. In addition, different results can be obtained depending on the method used to obtain the starting $\text{Mg}(\text{BH}_4)_2$ powders. Chlopek et al. [3], from their *in situ* temperature-resolved XRD studies at temperatures up to 753 K, had observed the formation of Mg and subsequently, MgB_2 , but when $\text{Mg}(\text{BH}_4)_2$ was heated up to 663 K under vacuum and quenched to room temperature, a mixture consisting of MgH_2 , Mg and MgB_4 were formed [3].

The residue material obtained from the vaporization experiment was a brownish-black powder dotted with black crystals suggesting the presence of some B, MgB_2 or some other form of B compounds. These compounds could not be detected from XRD since this profile showed that amorphous material was present, hence the B compounds could be present in amorphous form. The possibility of amorphous material present during and at the end of complete vaporization of $\text{Mg}(\text{BH}_4)_2$ has been reported [28,30,32,34,37]. The absence of peaks of crystalline material in this residue as opposed to the Mg observed in the residue of our first $\text{Mg}(\text{BH}_4)_2$ vaporization experiment suggests that the

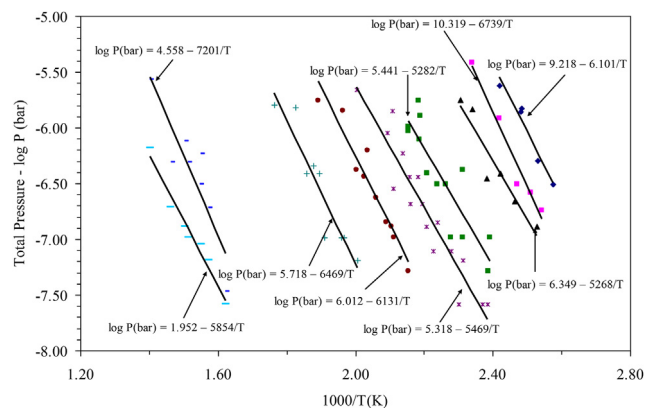


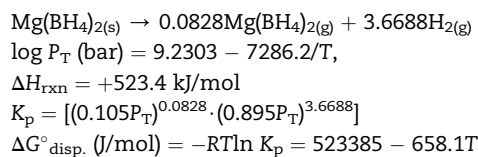
Fig. 10 – Complete vaporization analysis of $\text{Mg}(\text{BH}_4)_2$ from 388.2 K to 712.8 K using the torsion-effusion and gravimetry.

process of vaporization of $\text{Mg}(\text{BH}_4)_2$ as well as the nature of the starting material strongly influences the product outcome of dehydrating or decomposition.

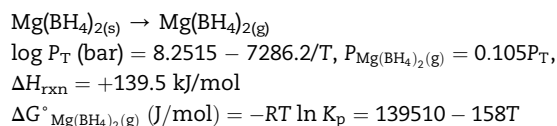
Summary of Measured Thermodynamic Parameters

A summary of the data obtained using crystalline samples are given below:

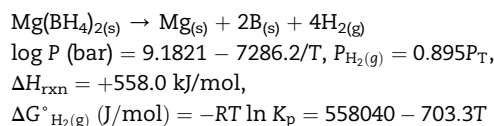
Disproportionation of $\text{Mg}(\text{BH}_4)_2 < 533$ K:



Sublimation of $\text{Mg}(\text{BH}_4)_2 < 533$ K:



Decomposition of $\text{Mg}(\text{BH}_4)_2 \geq 540$ K:



A comparison of thermodynamic data from the literature and this study are summarized in van't Hoff plots shown in Fig. A-2 in the Appendix. Graphical representations of various sets of data obtained from the decomposition of $\text{Mg}(\text{BH}_4)_2$, MgH_2 and Mg in their respective temperature ranges from this study and from other investigators [17,21,29,47,48]. The vapor pressures from listing of Equation Nos. 1, 2 and 3 [17,21,29] are higher most probably from the method used in obtaining these pressures. Our data and plots obtained from carefully raising the temperature of the system in a torsion-effusion gravimetric instrument that fall between van't Hoff plots for MgH_2 [47] and Mg [48]. The dehydrating enthalpies for $\text{Mg}(\text{BH}_4)_2$ from studies done in references [17,21,29] are -40.1 kJ/mol H_2 , -56.4 kJ/mol H_2 and -482.1 kJ/mol H_2 , respectively (this value was seen as unreasonable by the authors and said to arise from kinetic restrictions from the dehydrating process of $\text{Mg}(\text{BH}_4)_2$). Enthalpy values for the combined data from our studies of the dehydrating process of crystalline α - $\text{Mg}(\text{BH}_4)_2$ and crystalline β - $\text{Mg}(\text{BH}_4)_2$ with catalyst represented by equations No. 5 and No. 6 (Fig. A-2) are 142.3 and 120.6 kJ/mol, respectively. Enthalpy values for the high temperature (498–712 K) vapor pressure studies of amorphous $\text{Mg}(\text{BH}_4)_2$ starting material for equations Nos. 8 a, b & c are 123.9, 137.9 and 112.1 kJ/mol respectively. These enthalpies are obtained from the slopes of the Van't Hoff plots.

4. Conclusions

Vaporization studies on α , β , and amorphous $\text{Mg}(\text{BH}_4)_2(s)$ showed measurable vaporization in the temperature range of ~ 438 K to ~ 533 K, with disproportionation to (majority) H_2 gas and some small amounts of $\text{Mg}(\text{BH}_4)_2(s)$ with $\Delta H^\circ = 523$ kJ/mol.

Thermodynamic analyses yielded partial pressures, P_{H_2} (438 K) = 4×10^{-8} bar with $\Delta G^\circ_{438\text{K}} = 327$ kJ/mol, and P_{H_2} (533 K) = 3.2×10^{-5} bar with $\Delta G^\circ_{533\text{K}} = 235$ kJ/mol. Above ~ 540 K, vigorous decomposition to H_2 gas with condensed phase of Mg were observed, and we propose that boron metal is also present but in amorphous state; with $\Delta H^\circ = 558$ kJ/mol. The P_{H_2} (540 K) = 4×10^{-8} bar with $\Delta G^\circ_{540\text{K}} = 178$ kJ/mol, and P_{H_2} (773 K) = 5.64 bar with $\Delta G^\circ_{773\text{K}} = 14$ kJ/mol. The behavior of the amorphous $\text{Mg}(\text{BH}_4)_2(\text{s})$ was very different from those for the two crystalline phases (α and β), shows that at least five different steps are involved in the dehydrating pathway of $\text{Mg}(\text{BH}_4)_2$.

Acknowledgement

We greatly appreciate the financial support of the Intel Corporation. We particularly acknowledge, Murli Tirumala and Daryl Nelson for simulating discussions. We also thank Setaram Instruments for helping us with TGA experiments.

Appendix

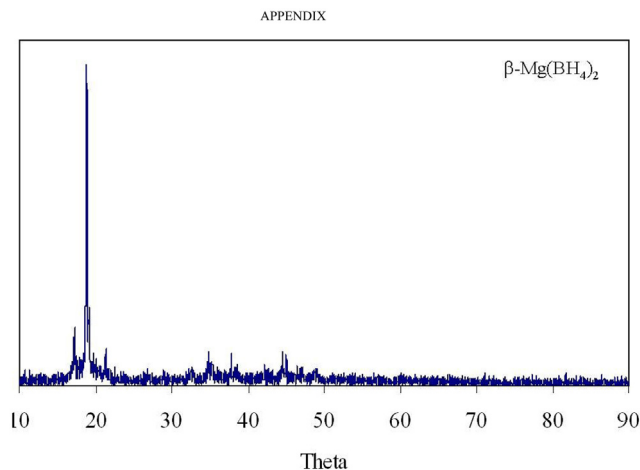


Fig. A-1. X-ray diffraction pattern of $\beta\text{-Mg}(\text{BH}_4)_2$ after heating $\alpha\text{-Mg}(\text{BH}_4)_2$ to 489 K.

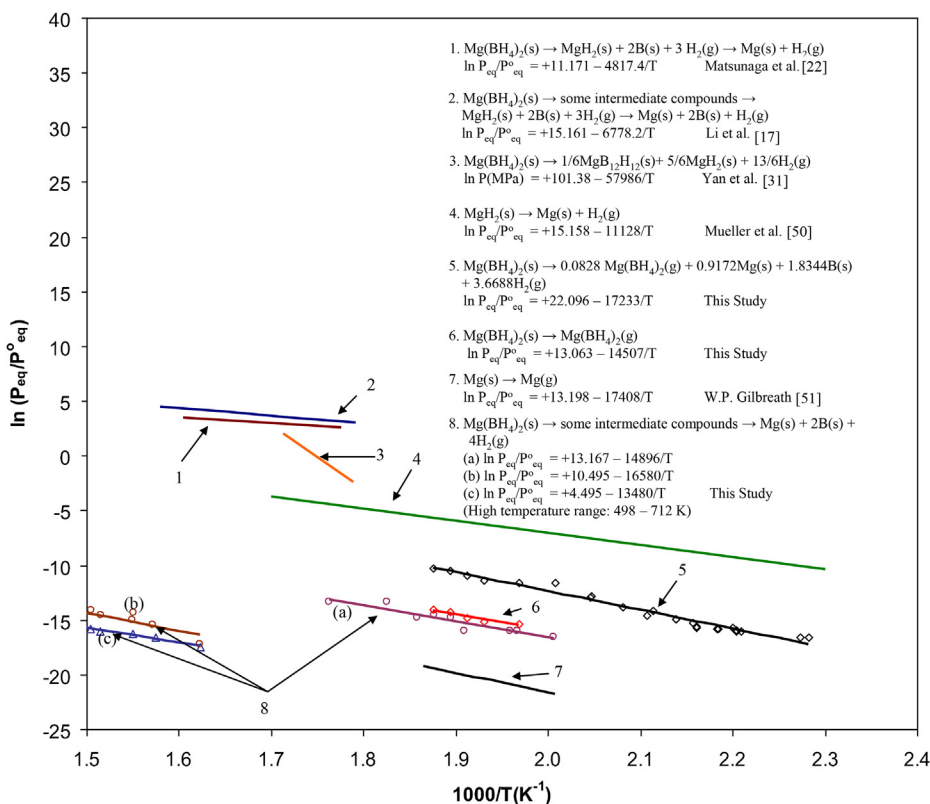


Fig. A-2. Summary of Van't Hoff plots as a function of inverse temperature for the dehydrating of crystalline $\alpha\text{-Mg}(\text{BH}_4)_2$ and crystalline $\beta\text{-Mg}(\text{BH}_4)_2$ with catalyst (Eq. Nos 5 and 6), amorphous $\text{Mg}(\text{BH}_4)_2$ (Eq. Nos. 8a, b, c), MgH_2 (Eq. Nos. 4, Ref. [47]), Mg (Eq. Nos. 7, Ref. [47]) and reports from other investigators (Eq. Nos. 1, 2 & 3, references [17,21,29], respectively).

Table A-3 – Total vapor pressures (P_T) for the complete vaporization analysis of $Mg(BH_4)_2$ from 115.2 °C to 439.8 °C using the torsion-effusion and thermogravimetry.

T (K)	Wt. Loss (mg/h)	P_T (bar)	MW (g/mol)	T (K)	Wt. Loss (mg/h)	P_T (bar)	MW (g/mol)
388.34		3.11E-07		467.88	0.034	5.97E-07	2.8
393.15		1.82E-07		473.21		1.04E-07	
395.02		5.06E-07		474.13		2.86E-07	
395.64		1.3E-07		474.44	0.111	1.42E-06	5.5
398.31		2.6E-07		474.79		1.3E-07	
402.71		1.5E-06		477.59	0.096	9.07E-07	
403.22		1.4E-06		478.51		1.43E-07	
404.85		3.11E-07		485.24		2.34E-07	
405.76		2.21E-07		491.14	0.043	6.23E-07	4.3
412.97		3.89E-07		493.31		3.63E-07	
413.28	0.119	2.39E-06	1.9	498.47		6.49E-08	
413.50		1.2E-06		498.81		4.15E-07	
417.98		1.04E-07		499.19	0.108	2.19E-06	2.3
419.00		5.19E-08		508.35		1.04E-07	
419.56		2.6E-08		508.89	0.108	1.42E-06	5.5
419.93		3.5E-07		510.40		1.04E-07	
422.03		2.6E-08		523.65		1.04E-07	
427.31	0.075	1.47E-06	2.1	527.67		3.89E-07	
427.51	0.182	3.82E-06	1.8	528.58	0.093	1.76E-06	2.8
432.20		1.04E-07		532.75		4.54E-07	
432.60		4.15E-07		538.10		3.89E-07	
432.60		6.49E-08		547.92	0.052	1.53E-06	1.2
433.63	0.098	1.78E-06	2.5	567.05	0.061	1.6E-06	1.5
434.79		2.6E-08		567.31		4.93E-07	
438.72		1.04E-07		576.60		4.67E-07	
438.72		7.79E-08		586.61	0.055	9.86E-07	3.4
442.05		3.11E-07		610.73		1.08E-06	
446.60		1.43E-07		616.11		2.59E-08	
446.62		3.11E-07		616.26		3.37E-08	
449.00		7.79E-08		635.11		6.49E-08	
452.58		3.89E-07		635.34		1.35E-06	
453.39		1.3E-07		636.04		1.89E-07	
455.56		2.08E-07		644.90	0.045	5.84E-07	7.2
457.04		1.27E-06		645.09		9.08E-08	
457.52		7.78E-07		645.44		3.11E-07	
457.69		1.76E-06		660.02		4.85E-07	
458.17		3.63E-07		660.15		1.04E-07	
463.30		2.08E-07		664.34		7.53E-07	
463.43		3.63E-07		664.99		1.3E-07	
463.91		5.19E-08		683.18		4.88E-07	
464.04	0.060	1.01E-06	3.1	683.52		1.95E-07	
464.04		9.33E-07		712.81	0.102	2.69E-06	1.9
				712.89		6.62E-07	
						AVG MW	3.12

REFERENCES

- [1] Wiberg E, Bauer R. *Z Naturforsch B* 1950;5:397–8.
- [2] Konoplev VN, Bakulina V. Some properties of magnesium borohydride. *Bull Acad Sci USSR Div Chem Sci (Engl Transl)* 1971;20:136–8.
- [3] Chłopek K, Frommen C, Léon A, Zabara O, Fichtner M. Synthesis and properties of magnesium tetrahydroborate, $Mg(BH_4)_2$. *J Mater Chem* 2007;17:3496–503.
- [4] Li H-W, Kikuchi K, Nakamori Y, Miwa K, Towata S, Orimo S. Effects of ball milling and additives on dehydriding behaviors of well-crystallized $Mg(BH_4)_2$. *Scripta Mater* 2007;57:679–82.
- [5] Riktor MD, Sørby MH, Chłopek K, Fichtner M, Buchter F, Züttel A, et al. *In situ* synchrotron diffraction studies of phase transitions and thermal decomposition of $Mg(BH_4)_2$ and $Ca(BH_4)_2$. *J Mater Chem* 2007;17:4939–42.
- [6] Černý R, Filinchuk Y, Hagemann H, Yvon K. Magnesium borohydride: synthesis and crystal structure. *Angew Chem Int Ed* 2007;46:5765–7 [Also published as Černý R, Filinchuk Y, Hagemann H, Yvon K. Magnesium borohydride: synthesis and crystal structure. *Angew Chem* 2007;119:5867–9].
- [7] Her J-H, Stephens PW, Gao Y, Soloveichik GL, Rijssenbeek J, Andrus M, et al. Structure of unsolvated magnesium borohydride $Mg(BH_4)_2$. *Acta Cryst B* 2007;63:561–8.
- [8] Dai B, Sholl DS, Johnson JK. First-principles study of experimental and hypothetical $Mg(BH_4)_2$ crystal structures. *J Phys Chem C* 2008;112:4391–5.
- [9] Filinchuk Y, Černý R, Hagemann H. Insight into $Mg(BH_4)_2$ with synchrotron X-ray diffraction: structure revision, crystal chemistry, and anomalous thermal expansion. *Chem Mater* 2009;21:925–33.

- [10] George L, Drozd V, Bardaji EG, Fichtner M, Saxena SK. Structural phase transitions of $\text{Mg}(\text{BH}_4)_2$ under pressure. *J Phys Chem C* 2009;113:486–92.
- [11] Filinchuk Y, Richter B, Jensen TR, Dmitriev V, Chenryshov D, Hagemann H. *Angew Chem Int Ed* 2011;50:11162–6.
- [12] Nakamori Y, Miwa K, Ninomiya A, Li H, Ohba N, Towata S, et al. Correlation between thermodynamical stabilities of metal borohydrides and cation electronegativities: first-principles calculations and experiment. *Phys Rev B* 2006;74:045126(1)–045126(9).
- [13] Vajeeston P, Ravidran P, Kjekshus A, Fjellvag H. High hydrogen content complex hydrides: a density-functional study. *Appl Phys Lett* 2006;89:071906(1)–071906(3).
- [14] Ozolins V, Majzoub EH, Wolverton C. First-principles prediction of a ground state crystal structure of magnesium borohydride. *Phys Rev Lett* 2008;100:135501(1)–135501(4).
- [15] van Setten MJ, de Wijs GA, Fichtner M, Brocks G. A density functional study of $\alpha\text{-Mg}(\text{BH}_4)_2$. *Chem Mater* 2008;20:4952–6.
- [16] Voss J, Hummelshj JS, Lodziana Z, Vegge T. Structural stability and decomposition of $\text{Mg}(\text{BH}_4)_2$ isomorphs – an ab initio free energy study. *J Phys Condens Matter* 2009;21:012203–9.
- [17] Li H-W, Kikuchi K, Sato T, Nakamori Y, Ohba N, Aoki M, et al. Synthesis and hydrogen storage properties of a single-phase magnesium borohydride $\text{Mg}(\text{BH}_4)_2$. *Mater Trans* 2008;49:2224–8.
- [18] van Setten MJ, Lohstroh W, Fichtner MA. New phase in the decomposition of $\text{Mg}(\text{BH}_4)_2$: first-principles simulated annealing. *J Mater Chem* 2009;19:7081–7.
- [19] Caputo R, Tekin A, Sikora W, Züttel A. First-principles determination of the ground-state structure of $\text{Mg}(\text{BH}_4)_2$. *Chem Phys Lett* 2009;480:203–9.
- [20] Zhou X-F, Qian Q-R, Zhou J, Xu B, Tian Y, Wang H-T. Crystal structure and stability of magnesium borohydride from first principles. *Phys Rev B* 2009;79:212102–5.
- [21] Matsunaga T, Buchter F, Mauron P, Bielman M, Nakamori Y, Orimo S, et al. Hydrogen storage properties of $\text{Mg}(\text{BH}_4)_2$. *J Alloys Compds* 2008;459:583–8.
- [22] Matsunaga T, Buchter F, Miwa K, Towata S, Orimo S, Züttel A. Magnesium borohydride: a new hydrogen storage material. *Renew Energy* 2008;33:193–6.
- [23] Soloveichik GL. Metal borohydrides as hydrogen storage materials. *Mater Matters* 2007;2:11–5.
- [24] Li H-W, Miwa K, Ohba N, Fujita T, Sato T, Yan Y, et al. Formation of intermediate compound with $\text{B}_{12}\text{H}_{12}$ cluster: experimental and theoretical studies on magnesium borohydride $\text{Mg}(\text{BH}_4)_2$. *Nanotechnology* 2009;20:204013–9.
- [25] Li H-W, Kikuchi K, Nakamori Y, Ohba N, Miwa K, Towata S, et al. Dehydriding and rehydriding processes of well-crystallized $\text{Mg}(\text{BH}_4)_2$ accompanying with formation of intermediate compounds. *Acta Mater* 2008;56:1342–7.
- [26] Hwang SJ, Bowman RC, Reiter JW, Rijssenbeek J, Soloveichik GL, Zhao JC, et al. NMR confirmation for formation of $[\text{B}_{12}\text{H}_{12}]^{2-}$ complexes during hydrogen desorption from metal borohydrides. *J Phys Chem C* 2008;112:3164–9.
- [27] Ozolins V, Majzoub EH, Wolverton C. First-principles prediction of thermodynamically reversible hydrogen storage reactions in the Li-Mg-Ca-B-H system. *J Am Chem Soc* 2009;131:230–7.
- [28] Hanada N, Chlopek K, Frommen C, Lohstroh W, Fichtner M. Thermal decomposition of $\text{Mg}(\text{BH}_4)_2$ under he flow and H_2 pressure. *J Mater Chem* 2008;18:2611–4.
- [29] Yan Y, Li H-W, Nakamori Y, Ohba N, Miwa K, Towata S, et al. Differential scanning calorimetry measurements of magnesium borohydride $\text{Mg}(\text{BH}_4)_2$. *Mater Trans* 2008;49:2751–2.
- [30] Soloveichik GL, Gao Y, Rijssenbeek J, Andrus M, Kniajanski S, Bowman Jr RC, et al. Magnesium borohydride as a hydrogen storage material: properties and dehydrogenation pathway of unsolvated $\text{Mg}(\text{BH}_4)_2$. *Int J Hydrogen Energy* 2009;34:916–28.
- [31] Severa G, Rönnebro E, Jensen CM. Direct hydrogenation of magnesium boride to magnesium borohydride – demonstration of >11 weight percent reversible hydrogen storage. *Chem Commun* 2010;46:421–3.
- [32] Newhouse RJ, Stavila V, Hwang S-J, Klebanoff LE, Zhang JZ. Reversibility and improved hydrogen release of magnesium borohydride. *J Phys Chem C* 2010;114:5224–32.
- [33] Kim KC, Allendorf MD, Stavila V, Sholl DS. Predicting impurity gases and phases during hydrogen evolution from complex metal hydrides using free energy minimization enabled by first-principles calculations. *Phys Chem Chem Phys* 2010;12:9918–26.
- [34] Kulkarni A, Wang L-L, Johnson DD, Sholl D, Johnson K. First-principles characterization of amorphous phases of $\text{MB}_{12}\text{H}_{12}$, $\text{M} = \text{Mg, Ca}$. *J Phys Chem C* 2010;114:14601–5.
- [35] Li S, Willis M, Jena P. Reaction intermediates during the dehydrogenation of metal borohydrides – a cluster perspective. *J Phys Chem C* 2010;114:16849–54.
- [36] Chong M, Karkamkar A, Autrey T, Orimo S, Jalisatgi S, Jensen CM. Reversible dehydrogenation of magnesium borohydride to magnesium triborane in the solid state under moderate conditions. *Chem Commun* 2011;47:1330–2.
- [37] Zhang ZG, Luo FP, Wang H, Liu JW, Zhu M. Direct synthesis and hydrogen storage characteristics of Mg-B-H compounds. *Int J Hydrogen Energy* 2012;37(1):926–31.
- [38] Varin RA, Chiu Ch, Wronski ZS. Mechano-chemical activation synthesis (MCAS) of disordered $\text{Mg}(\text{BH}_4)_2$ using NaBH_4 . *J Alloys Compds* 2008;462:201–8.
- [39] Hagemann H, Černý R. Synthetic approaches to inorganic borohydrides. *Dalton Trans* 2010;39:6006–12 [Also see Hagemann H, D'Anna V, Rapin J-P, Yvon K. Deuterium-hydrogen exchange in solid $\text{Mg}(\text{BH}_4)_2$. *J Phys Chem C* 2010;114:10045–7].
- [40] Margrave J. Characterization of high temperature vapors. NY: John Wiley and Sons Inc.; 1967. p. 48–55, 74–75, 91–95, 115–143.
- [41] Chandra D, Lau KH, Chien W, Garner M. Torsion effusion vapor pressure determinations of Os, Rh, Ru, W, Co, and Cr solid carbonyls. *J Phys Chem Solids* 2005;66:241–5.
- [42] Chien W-M, Chandra D, Lau KH, Hildenbrand DL, Helmy AM. The vaporization of NH_4NO_3 . *J Chem Thermodyn* 2010;42:846–51.
- [43] Lau KH, Cubicciotti D, Hildenbrand DL. Effusion studies of the thermal decomposition of magnesium and calcium sulfates. *J Chem Phys* 1977;66:4532–9.
- [44] Hildenbrand DL, Knight DL. Composition of saturated beryllium chloride vapor. *J Chem Phys* 1969;51:1260–6.
- [45] Garner ML, Chandra D, Lau KH. Vapor pressures of osmium, rhodium, and ruthenium carbonyls. *J Phase Equilibria* 1999;20:565–72.
- [46] Garner ML, Chandra D, Lau KH. Low-temperature vapor pressures of W-, Cr-, and Co-carbonyls. *J Phase Equilibria* 1995;16:24–9.
- [47] Gilbreath WP. The vapor pressure of magnesium between 233 and 385 °C. Report No. NASA TND-2733 (Archival No. 20011130 130). Moffitt Field, CA: NASA Ames Research Lab; 1985.
- [48] Mueller WM, Blackledge JP, Libowitz GG. Metal hydrides. New York: Academic; 1968. p. 555.
- [49] Greatrex R, Greenwood NN. Kinetics of boron hydride interconversion reactions. Final report; May 1986–Sep 1989. p. 96 [and references therein].